Supplementary Information

Table S1: Run conditions and major element analyses of metal and silicate phases (all experiments at 1 GPa)

Sample	150	160B§	170	180F	190F	160-30§	160-60§	160-120§	164	166	1610 B	184D	186D	1810 C	160m	164m	166m	168m	1610m
Temperature (°C)	1500	1600	1700	1800	1900	1600	1600	1600	1600	1600	1600	1800	1800	1800	1600	1600	1600	1600	1600
Duration (min)	180	90	45	15	15	30	60	120	90	90	90	15	15	15	90	90	90	90	90
capsule	C	C	C	C	C	C	C	C	C	C	C	C	C	C	MgO	MgO	MgO	MgO	MgO
Silicate (n)	25	30	25	40	45	25	25	25	30	20	25	35	35	40	40	50	40	50	40
SiO_2	38.3	36.4	37.9	35.7	37.7	38.8	37.6	38.6	47.1	53.7	55.1	54.2	55.8	52.4	28.36	43.41	39.83	39.59	39.06
TiO_2	3.20	3.01	3.17	2.96	3.20	3.26	3.15	3.30	3.13	3.01	0.50	3.38	3.00	2.25	3.48	7.32	3.32	2.16	1.65
Al_2O_3	10.5	14.5	11.3	9.4	9.8	9.0	11.3	9.2	18.1	10.5	13.4	11.5	11.4	12.4	10.79	11.98	12.8	13.41	12.89
Cr_2O_3	-	-	-	0.06	0.05	-	-	-	-	-	-	0.01	0.01	-	-	-	-	-	-
FeO	17.45	17.24	17.59	18.17	17.34	17.84	17.83	16.42	0.20	0.08	0.01	0.47	0.19	0.09	12.12	0.11	0.045	0.017	0.01
MnO	0.18	0.18	0.20	0.18	0.19	0.20	0.19	0.19	0.15	0.14	0.08	0.18	0.15	0.07	0.15	1.61	0.086	0.03	0.026
CaO	10.87	10.32	10.84	10.27	10.83	10.85	10.77	11.15	11.21	12.99	12.35	12.27	12.12	12.01	11.89	7.19	13.08	13.63	12.85
MgO	12.9	12.3	13.2	12.2	12.7	13.6	12.5	14.0	13.0	14.4	13.8	13.6	13.4	17.1	26.46	21.99	25.67	28.36	26.01
Na_2O	2.49	2.47	2.63	2.60	2.58	2.52	2.67	2.67	2.56	2.32	2.78	2.84	2.59	3.09	3.38	3.5	3.6	3.69	3.57
K_2O	1.30	1.31	1.32	1.46	1.43	1.33	1.39	1.33	1.54	1.55	1.71	1.79	1.74	1.58	1.91	2.06	2.21	2.21	2.12
P_2O_5	0.69	0.58	0.70	0.70	0.59	0.78	0.68	0.70	0.02	0.02	0.02	0.01	0.01	0.01	0.81	0.08	0.02	0.03	0.02
SO_2	0.41	0.45	0.40	0.73	0.78	0.51	0.41	0.40	1.01	1.68	1.62	1.12	1.69	1.62	-	-	-	-	-
BaO	0.03	0.03	0.02	3.84	0.88	0.03	0.03	0.05	0.03	0.00	0.06	0.04	0.22	0.07	-	-	-	-	-
In_2O_3	-	-	-	0.61	0.60	-	-	-	-	-	-	0.17	0.07	-					
Total	98.25	98.78	99.26	98.82	98.68	98.72	98.53	98.08	98.11	100.39	101.41	101.55	102.34	102.69	99.35	99.25	100.66	101.13	98.21
As ppm	0.75	0.61	2.07	1.93	2.29	0.83	1.30	0.77	0.47	1.52	4.16	2.10	3.43	17.67	-	0.77	4.47	28.22	14.90
Sb ppm	9.65	7.97	19.8	23.6	28.0	10.6	16.0	10.2	0.04	0.42	1.15	1.62	1.97	9.55	10.60	0.11	1.19	7.37	7.37
Ge ppm	134	108	219	286	323	138	118	126	1.34	2.27	2.46	5.48	4.03	4.38	93.63	-	-	-	-
In ppm	9189	788	4202	4900	5400	3067	1413	14434	1114	101	756	1218	234	953	1670	71.5	44.5	189	163

Metal (n)	35	40	35	25	15	30	15	20	25	11	20	25	20	31	40	50	40	50	40
Fe	82.79	82.95	85.73	84.87	86.59	83.68	82.46	79.30	86.41	85.67	79.92	85.05	84.91	78.01	87.81	89.53	86.51	80.13	78.01
P	0.09	0.11	0.06	0.067	0.11	0.12	0.06	0.10	0.52	0.89	0.86	0.88	0.80	0.92	0.14	0.89	0.76	0.78	0.87
S	1.65	2.13	1.52	1.38	0.99	1.95	1.54	1.98	0.20	0.32	0.03	0.57	0.43	0.02	1.57	0.64	0.11	0	0
C	4.25	4.26	4.80	4.87	5.28	4.07	2.38	5.16	5.25	3.98	1.66	5.95	4.79	1.97	0	0	0	0	0
Si	0.06	0.04	0.03	0.024	0.03	0.02	0.01	0.03	0.92	4.17	13.49	0.61	4.61	13.85	0.01	1.25	5.94	13.47	13.69
As	3.14	3.28	3.07	2.66	3.05	4.06	3.83	4.71	1.32	1.62	1.58	2.00	1.99	1.74	2.07	1.57	1.3	1.34	1.48
Sb	2.45	2.74	2.21	1.99	2.32	2.66	4.06	4.09	1.05	1.74	0.40	1.71	1.62	0.97	2.2	1.68	1.3	1.07	1.03
Ge	3.64	3.61	3.46	3.54	3.15	2.46	4.43	2.83	2.36	1.84	1.06	2.16	1.80	1.93	3.08	2.11	1.8	1.42	1.5
In	0.86	0.15	0.20	0.047	0.04	0.62	0.26	2.10	0.64	0.09	0.36	0.14	0.08	0.06	1.81	0.8	0.35	0.68	0.68
Total	98.93	99.27	101.81	99.45	101.56	99.64	99.04	100.30	98.67	100.31	99.36	99.07	101.27	99.47	98.69	98.40	98.07	98.89	97.20
lnK_d (Fe-As)-1/2 lnγFe	10.1	13.4	3.3	3.7	3.0	15.7	8.8	21.2	5.8E-6	2.0E-7	1.2E-9	8.6E-5	3.0E-6	1.0E-7	-	2.27E-07	2.50E-09	7.97E-11	4.84E-11
	+2.4	+3.2	+0.5	+0.5	+0.4	+4.0	+1.8	+3.6	+0.70 E-6	0.58E-7	+0.7E-9	+2.4E-5	+1.1E-6	+0.3E-7	-	+0.3 E-07	+0.4 E-09	+1.1 E-11	+0.6 E-11
	-2.2	-3.0	-0.6	-0.5	+0.5	-4.2	-1.9	-3.5	-0.76E-6	-0.65E-7	-0.8E-9	-2.2E-5	-0.9E-6	-0.4E-7	-	-0.4 E-07	-0.5 E-09	-0.9 E-11	-0.5 E-11
lnK_d (Fe-Sb)-1/2 lnγFe	0.44	0.57	0.19	0.17	0.14	0.69	0.40	0.89	3.50E-5	3.95E-7	2.40E-9	6.17E-5	2.93E-6	1.07E-7	2.64E-02	1.15E-06	5.78E-09	1.20E-10	2.92E-11
	+0.08	+0.09	+0.03	+0.03	+0.02	-0.11	+0.08	+0.15	+0.80 E-5	+0.88E-7	+0.40 E-9	+0.60 E-5	+0.45 E-6	+0.75 E-7	+0.4 E-02	+0.3 E-06	+0.9 E-09	+0.3 E-10	+0.6+0.3 E-
	-0.07	-0.08	-0.03	-0.03	-0.02	-0.10	-0.08	-0.14	-0.75E-5	-0.80E-7	-0.40E-9	-0.57E-5	-0.40E-6	-0.70E-7	-0.4 E-02	-0.25 E-06	-0.8 E-09	-0.3 E-10	-0.5+0.3 E-
lnK_d (Fe-Ge)	52.7	63.7	29.7	25.1	18.1	34.9	74.5	43.0	42.5	8.6	1.2	29.2	12.8	8.2	35.33	-	-	-	-
	+11.0	+14.0	+6.3	+5.2	+3.8	+7.4	+16.2	+9.2	+9.1	+5.2	+0.8	+6.4	+4.0	+2.6	+6.2	-	-	-	-
	-9.0	-11.0	-5.0	-4.2	-3.1	-5.9	-14.5	-7.3	-7.2	-3.1	-0.6	-5.2	-3.1	-2.0	-5.8	-	-	-	-
lnK_d (Fe-In)-1/2 lnγFe	6.74E-4	2.33E-4	7.50E-5	3.83E-6	2.25E-6	1.06 E-3	4.28E-4	2.45E-3	3.72E-5	3.71E-6	1.92E-6	4.81E-6	2.89E-6	2.84E-7	1.06E-02	4.25E-04	5.75E-05	2.71E-05	1.98E-05
	+2.0E-4	+0.6E-4	+2.0E-5	+1.0E-6	+0.6E-6	+0.3 E-3	+1.2E-4	+0.6E-3	+1.4E-5	+2.3E-6	+1.4E-6	+1.4E-6	+1.1E-6	+1.2E-7	+0.3 E-02	+0.6 E-04	+0.7E-05	+0.3E-05	+0.4E-05
	-1.4E-4	-0.4E-4	-1.6E-5	-0.8E-6	-0.5E-6	-0.4E-3	-0.9E-4	-0.5E-3	-1.0E-5	-1.5E-6	-1.0E-6	-1.1E-6	-0.8E-6	-0.8E-7	-0.2 E-2	-0.5 E-04	-0.65E-05	-0.32E-05	-0.5E-05

ΔIW	-1.36 (3)	-1.35 (3)	-1.36 (3)	-1.25 (3)	-1.34 (3)	-1.35 (3)	-1.40 (3)	-1.36 (3)	-5.25 (11)	-6.08 (26)	-7.57 (42)	-4.28 (5)	-5.21 (11)	-5.92 (12)	-1.95 (17)	-6.01 (25)	-6.76 (28)	-7.50 (24)	-7.91 (35)	
ΔIW (a Fe)	-0.81 (3)	-0.81 (3)	-0.79 (3)	-0.66 (3)	-0.79 (3)	-0.80 (3)	-0.85 (3)	-0.81 (3)	-4.59 (11)	-5.36 (26)	-6.53 (42)	-3.60 (5)	-4.42 (11)	-4.58 (12)	-1.54	-5.60	-6.28	-6.72	-7.10	
NBO/T	1.64	1.63	1.64	1.65	1.64	1.82	1.62	1.76	0.69	0.96	0.83	0.70	1.00	0.80	2.75	1.26	1.73	1.89	1.79	
γFe	0.86	0.85	0.83	0.81	0.80	0.85	0.85	0.85	0.75	0.70	0.48	0.73	0.64	0.48	1.00	1.00	0.92	0.65	0.64	

Footnote: Error on EMPA analysis of metals and Ti, Fe, Mn, Ca and K in silicates is 2%, and on Si, Al, Mg, Na, P, and S is 5%. LA-ICP-MS error is 10%.

ΔIW and K_d/γFe error is based on uncertainty in measured Fe, As, Ge, Sb and In in glass and metal.

§ indicates part of the time series.

Figures S1

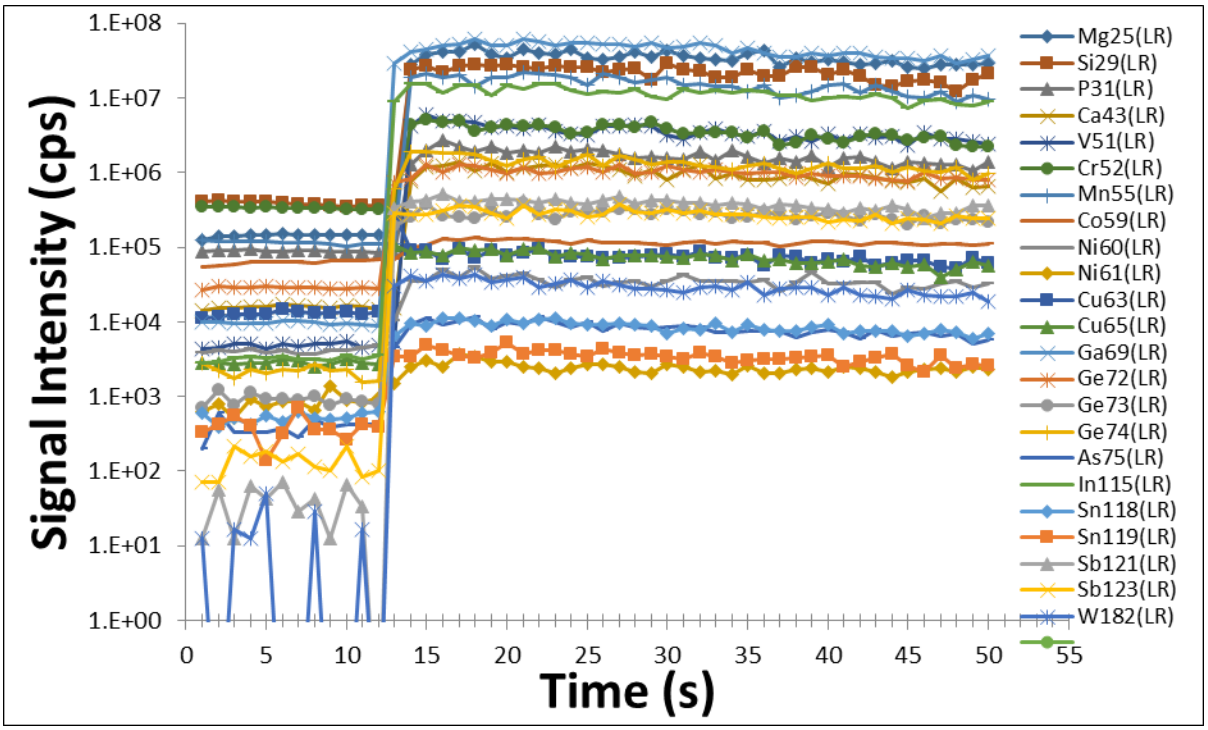

Figure S1A: example of a clean LA-ICP-MS analysis (experiment 180F) which exhibits strong signals for all trace elements and no interfering metallic particles at depth.

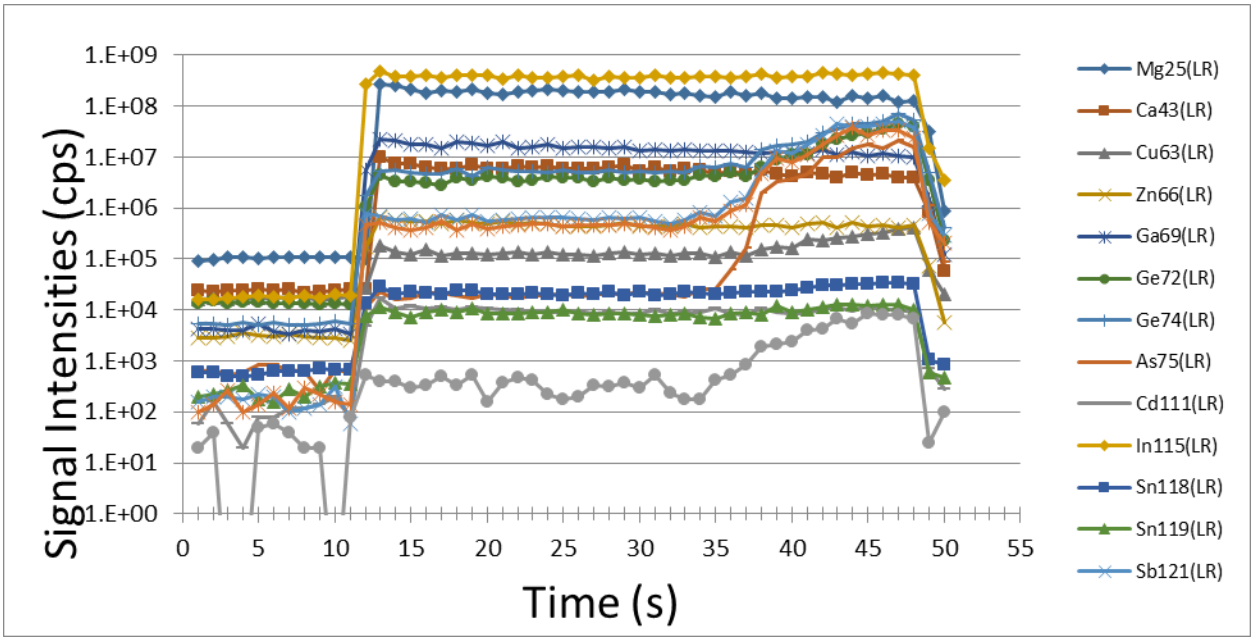

Figure S1B: example of a LA-ICP-MS analysis (experiment 190F) that is compromised by a metallic nugget at depth. In this case only the points between 15 and 30 sec are averaged to calculate the composition of the silicate.

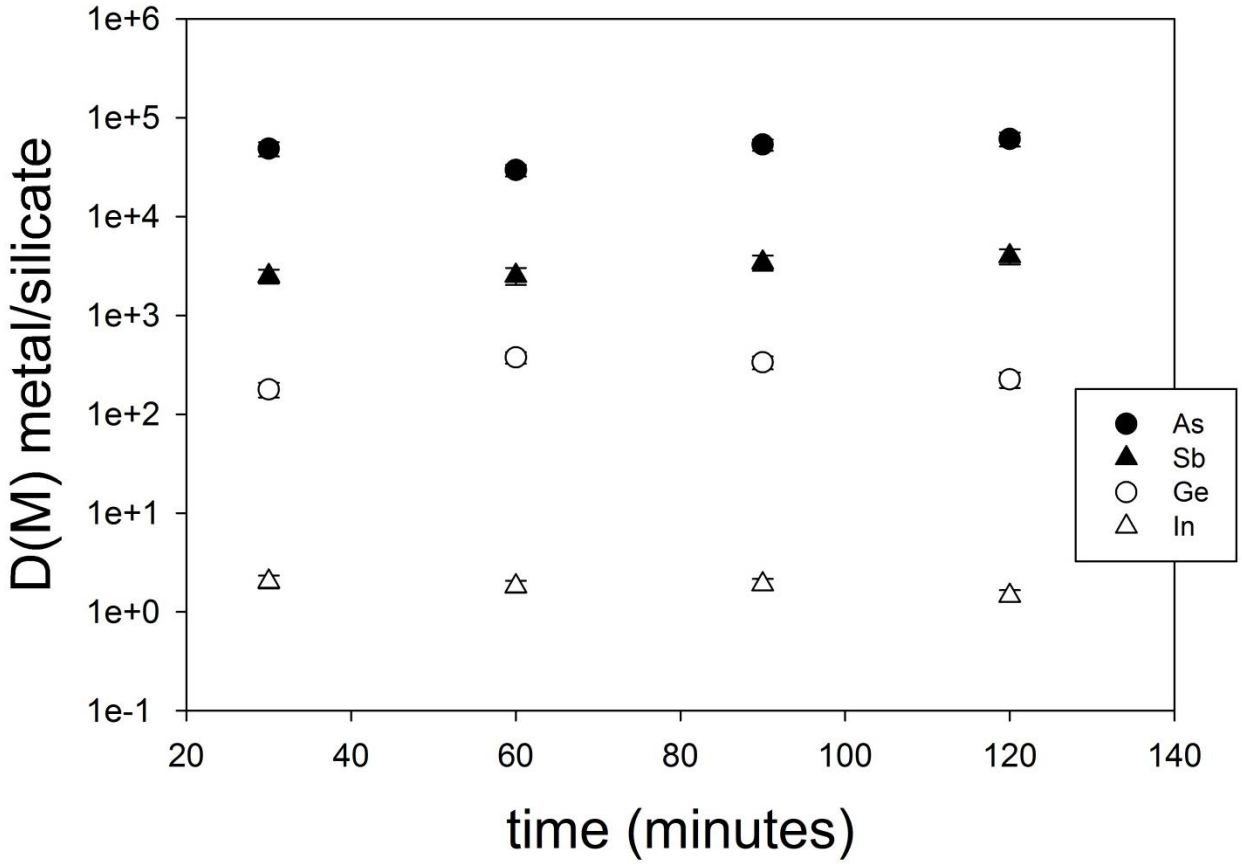

Fig. S2: Time series of metal-silicate partition coefficients for As, Sb, Ge, and In. All experiments carried out at 1600 °C and 1 GPa. Experiments were carried out at 30, 60, 90 and 120 minutes (Table S1; experiments 160-30, 160-60, 160B, and 160-120, respectively). The partition coefficient values do not change, outside of error on the analyses, after 60 minutes, indicating the equilibrium was approached.

Fig. S3: transect

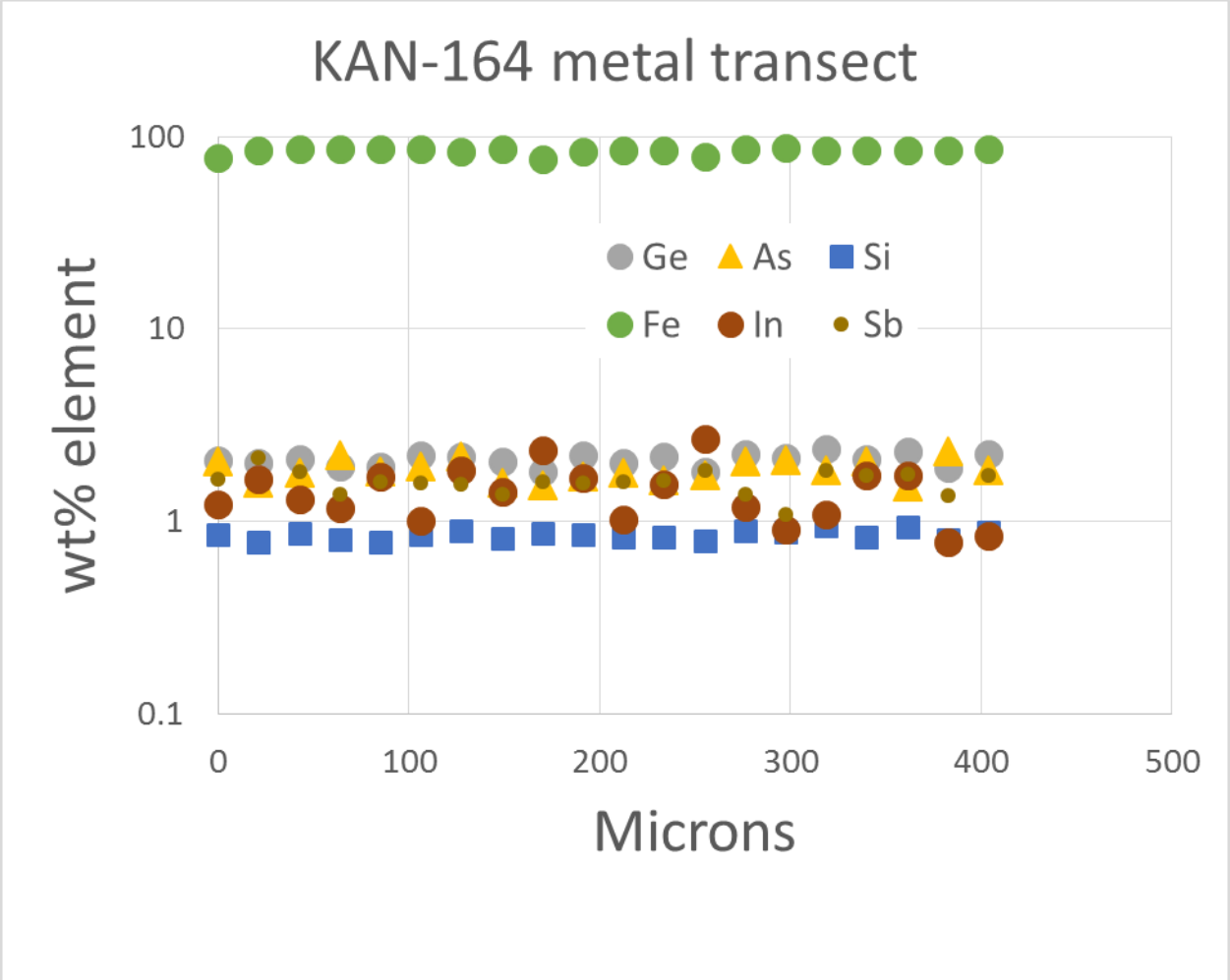

Fig. S3: Transect across a metallic sphere from experiment KAN-164. This transect was done over 400 microns, from edge to core of a metallic sphere, using a beam of 20 micron width at a spacing of ~21 microns between analyses. The metallic sphere quenched to a fine grained multi-phase matte; the broad beam analysis across this sample clearly shows homogeneity for all elements. Indium is more variable across the transect due to its affinity for some of the quench phases over the others, but show no trend or zoning across this long transect.

Table S2: Analytical details

ppm		As	Ge	In	Sb
BHVO2g[c]		0.81(12)	1.6(1)	0.10(2)	0.21(4)
BHVO2g – Rice		0.79(8)	1.6(2)	0.08(1)	0.18(2)
BHVO2g – UH		1.33(42)	1.07(29)	0.10(1)	0.15(2)
BCR2g[c]		1.1(1)	1.5(2)	0.11(1)	0.35(5)
BCR2g – Rice		0.95(9)	1.7(2)	0.09(1)	0.29(3)
NIST 610[a]		325(18)	447(78)	434(19)	396(19)
NIST 610 – Rice		338(34)	431(43)	425(43)	379(38)
NIST 610 - UH		341(32)	417(16)	447(17)	399(15)
NIST 612[b]		35.7(5.5)	36.1(3.8)	38.9(2.1)	34.7(1.8)
NIST 612 – Rice		34.5(3.4)	39.2(3.9)	37.2(3.7)	34.9(3.5)
NIST 612 - UH		35.7(3.4)	36.1(1.4)	38.9(1.5)	34.7(1.3)
180F - Rice		1.9(2)	286(29)	4900(490)	23.6(2.4)
180F - UH		2.56(63)	352(13)	4813(250)	32.6(3.0)
190F - Rice		2.3(2)	323(32)	5400(540)	28.0(3.0)
190F - UH		2.75(52)	306(13)	5870(210)	30.2(1.7)

a Pearce et al 1997; b - Pearce et al 1998; c - GEOREM values

fO_2 diagrams

A standard approach to examine the influence of oxygen fugacity on partition coefficients is to plot D(met/sil) vs. logfO_2, and D increases with decreasing fO_2 according to the valence of the element in question. For example, a 3+ element will have a slope of 0.75, 2+ a slope of 0.5, and 1+ a slope of 0.25. This approach cannot be used here for these elements, because the activity coefficients are so large that the slopes of D versus fO_2 do not yield any information about valence (Figure S4A,B and S5A,B). Our results show such trends at low Si contents, but at Si >2 wt%, D(met/sil) become much lower than expected, demonstrating a very large effect of dissolved Si into the metallic liquid (Figure S4A,B and S5A,B). When corrected for activity variation, using the activity moel of Ma (2001) and the epsilon parameters described in the text, As, Sb, and In all exhibit consistency with 3+, and Ge with 2+ cations in the silicate melt at both 1600 and 1800 °C (Figure S4C,D and S5C,D).

Activity model of Ma (2001):

$$\ln\gamma_i = \ln\gamma_{Fe} + \ln\gamma_i^0 - \varepsilon_i^i \ln(1-X_i) - \sum_{j=1(j\neq i)}^{N-1} \varepsilon_i^j X_j \left(1 + \frac{\ln(1-X_j)}{X_j} - \frac{1}{1-X}\right) + \sum_{j=1(j\neq i)}^{N-1} \varepsilon_i^j X_j^2 X_i \left(\frac{1}{1-X_i} + \frac{1}{1-X_j} + \frac{X_i}{2(1-X_i)^2} - 1\right)$$

where

$$\ln\gamma_{Fe} = \sum_{i=1}^{N-1} \varepsilon_i^i (X_i + \ln(1-X_i)) - \sum_{j=1}^{N-2}\sum_{k=j+1}^{N-1} \varepsilon_j^k X_j X_k \left(1 + \frac{\ln(1-X_j)}{X_j} + \frac{\ln(1-X_k)}{X_k}\right) + \sum_{i=1}^{N-1}\sum_{k=1(k\neq i)}^{N-1} \varepsilon_i^k X_i X_k \left(1 + \frac{\ln(1-X_k)}{X_k} - \frac{1}{1-X_i}\right) + \frac{1}{2}\sum_{j=1}^{N-2}\sum_{k=j+1}^{N-1} \varepsilon_j^k X_j^2 X_k^2 \left(\frac{1}{1-X_j} + \frac{1}{1-X_k} - 1\right) - \sum_{i=1}^{N-1}\sum_{k=1(k\neq i)}^{N-1} \varepsilon_i^k X_i^2 X_k^2 \left(\frac{1}{1-X_i} + \frac{1}{1-X_k} + \frac{X_i}{2(1-X_i)^2} - 1\right)$$

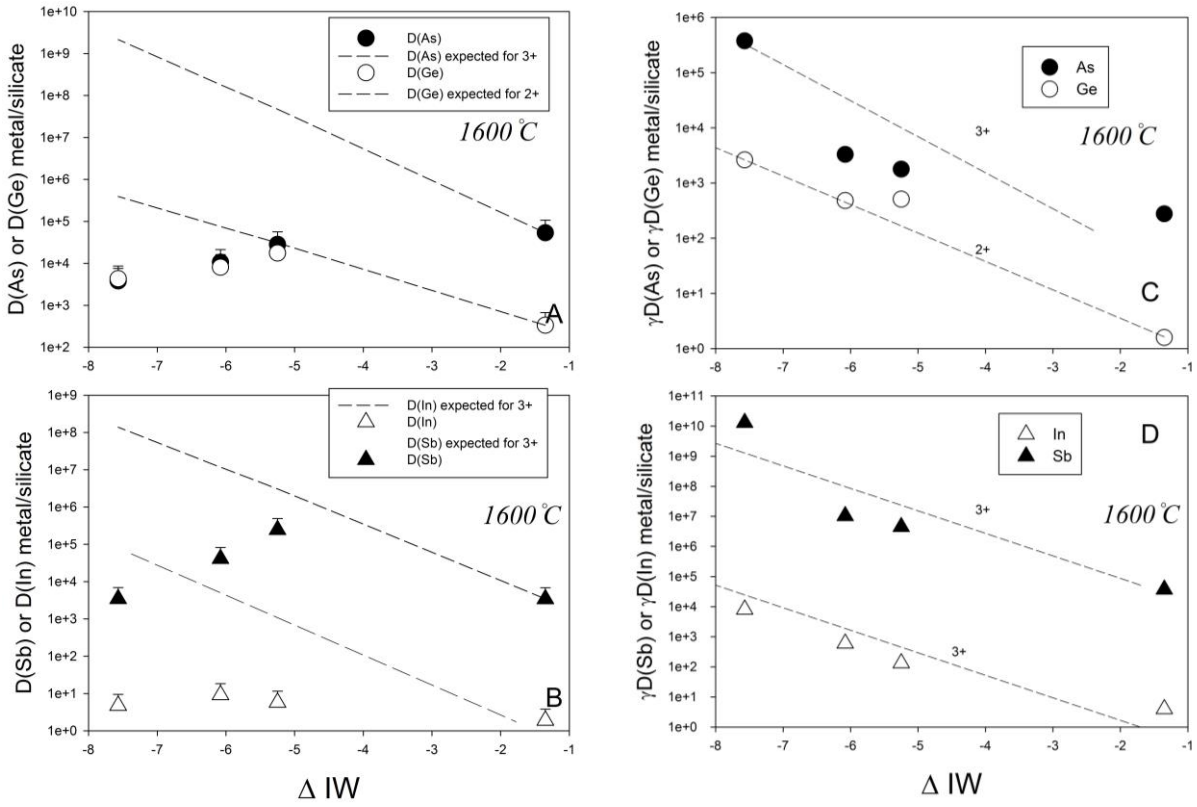

Fig. S4A: D(Ge) metal/silicate and D(As) metal/silicate versus ΔIW at 1600 °C. Dashed lines are the expected trends with oxygen fugacity for a 3+ (As) and 2+ (Ge) anion. Both As and Ge values plot lower than the expected trend due to the influence of Si alloyed in the metallic liquid. All D values are from Table S3. **Fig. S4B:** D(Sb) metal/silicate and D(In) metal/silicate versus ΔIW at 1600 °C. Dashed lines are the expected trends with oxygen fugacity for a 3+ (Sb) and 3+ (In) anion. Both Sb and In values plot lower than the expected trend due to the influence of Si alloyed in the metallic liquid. D(Sb) is much lower compared to D(In) indicating a stronger effect of Si on Sb. All D values are from Table S3. **Fig. S4C:** γD(Ge) metal/silicate and γD(As) metal/silicate versus ΔIW at 1600 °C. Dashed lines are the expected trends with oxygen fugacity for a 3+ (As) and 2+ (Ge) anion. When corrected for activity, As and Ge values plot along trends expected for 3+ and 2+ cations, respectively. **Fig. S4D:** γD(Sb) metal/silicate and γD(In) metal/silicate versus ΔIW at 1600 °C. Dashed lines are the expected trends with oxygen fugacity for a 3+ (Sb) and 2+ (In) anion. When corrected for activity, Sb and In values plot along trends expected for 3+ cations.

Activity coefficients calculated using the activity model of Ma (2001) with epsilon parameters from this work and other values from Wade and Wood (2006) and Wood et al. (2014).

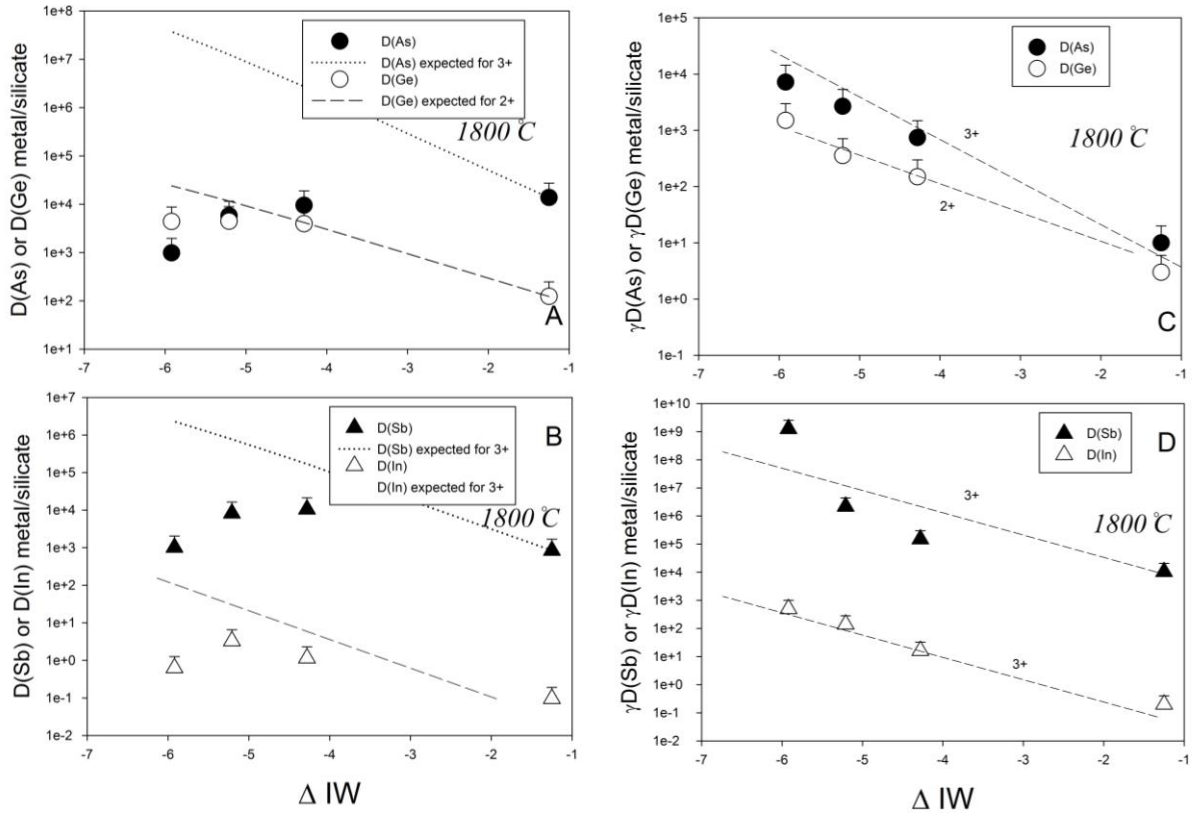

Fig. S5A: D(Ge) metal/silicate and D(As) metal silicate versus ΔIW at 1800 °C. Dashed lines are the expected trends with oxygen fugacity for a 3+ (As) and 2+ (Ge) anion. Both As and Ge values plot lower than the expected trend due to the influence of Si alloyed in the metallic liquid. All D values are from Table S3. **Fig. S5B:** D(Sb) metal/silicate and D(In) metal silicate versus ΔIW at 1800 °C. Dashed lines are the expected trends with oxygen fugacity for a 3+ (Sb) and 3+ (In) anion. Both Sb and In values plot lower than the expected trend due to the influence of Si alloyed in the metallic liquid. D(Sb) is much lower compared to D(In) indicating a stronger effect of Si on Sb. All D values are from Table S3. **Fig. S5C:** γD(Ge) metal/silicate and γD(As) metal/silicate versus ΔIW at 1800 °C. Dashed lines are the expected trends with oxygen fugacity for a 3+ (As) and 2+ (Ge) anion. When corrected for activity, As and Ge values plot along trends expected for 3+ and 2+ cations, respectively. **Fig. S5D:** γD(Sb) metal/silicate and γD(In) metal/silicate versus ΔIW at 1800 °C. Dashed lines are the expected trends with oxygen fugacity for a 3+ (Sb) and 2+ (In) anion. When corrected for activity, Sb and In values plot along trends expected for 3+ cations.

Activity coefficients calculated using the activity model of Ma (2001) with epsilon parameters from this work and other values from Wade and Wood (2006) and Wood et al. (2014).

Table S3: Run conditions and major element analyses of metal and silicate phases (all experiments at 1 GPa)

Sample	150	160B	170	180F	190F	160-30	160-60	160-120	164	166	1610B	184D	186D	1810	160m	164m	166m	168m	1610m
Temperat	1500	1600	170	180	1900	1600	1600	1600	1600	1600	1600	1800	1800	180	160	160	1600	1600	1600
Duration	180	90	45	15	15	30	60	120	90	90	90	15	15	15	90	90	90	90	90
D(As)	**4175**	**5350**	**1480**	**138**	**133**	**4870**	**2950**	**61090**	**28230**	**10630**	**3800**	**9510**	**5800**	**985**	**-**	**2039**	**2908**	**475**	**993**
	+750	+900	+250	+22	+22	+830	+500	+100		+1800	+600		+1000	+15	-	+250	+320	+62	+135
D(Sb)	**2540**	**3440**	**1100**	**840**	**830**	**2520**	**2530**	**4000**	**24530**	**41170**	**3470**	**10560**	**8240**	**1020**	**2075**	**1575**	**1092**	**1452**	**1398**
	+400	+550	+200			+450	+550		+6000	+7000	+600		+1300	+16	+260	+200	+140	+210	+200
D(Ge)	**272**	**335**	**158**	**124**	**98**	**180**	**376**	**225**	**17590**	**8100**	**4300**	**3950**	**4460**	**4400**	**329**	**-**	**-**	**-**	**-**
	+45	+55	+25	+20	+15	+30	+60	+40		+1300	+700	+650	+750	+70	+40	**-**	**-**	**-**	**-**
D(In)	**0.94**	**1.9**	**0.48**	**0.10**	**0.07**	**2.0**	**1.8**	**1.5**	**5.8**	**9.2**	**4.8**	**1.15**	**3.29**	**0.63**	**10.84**	**111.**	**78.6**	**35.9**	**41.8**
		+0.3				+0.4	+0.3	+0.2	+0.9	+1.2	+0.8	+0.20	+0.70	+0.1	+2.2	+16.	+10.	+5.6	+6.2

Table S4: Bulk and mantle concentrations of Ge, In, As, and Sb

	As (ppb)	Sb (ppb)	Ge (ppm)	In (ppb)
Earth Mantle [1]	27(4) 68(20)	5.4 (2.2)	1.2(2)	19(3)
CI chondrite [2]	1860	140	32	80
Earth bulk [3]	620	47	11	20
Volatility factor	3(±1)	3(±1)	3(±1)	4(±1)
50% condensation temperature (K)[4]	1065	979	883	800

1 - Palme and O'Neill (2014); Witt-Eickschen et al. (2009).

2 - from Newsom (1995)

3 - bulk Earth as CI chondrite and volatility corrected (see text).

4 – from Lodders (2003) except for In which was calculated as described in the text.

Table S5: Regression results for lnD' (metal/silicate) partition coefficients

	N	References	a ($lnfO_2$)	b (1/T)	c (P/T)	d (nbo/t)	e	R^2	2σ
Ge	85	[1,2,5,10-15]	-0.41 (4)	-24090 (2600)	680 (80)	-0.26 (11)	5.92 (01.17)	0.835	0.80
In	44	[1,3,4,16]	-1.07 (21)	-75860(15500)	1336(290)	0.09 (43)	20.7 (5.0)	0.753	1.65
As	33	[1,5]	-0.68 (37)	-18545(5860)	-42(122)	-0.24(6)	12.64(2.38)	0.854	1.02
Sb	51	[1,6,8,9,10]	-0.66(16)	-1700(1200)	2050(1020)	-0.73 (1.33)	-4.15 (1.23)	0.632	2.50

$\ln D'(M) = \ln D(M) - \ln\gamma(M)met = a\ln fO_2 + b/T + cP/T + d\,(nbo/t) + e$

References: [1] this study; [2] Righter et al. (2011); [3] Mann et al. (2009); [4] Ballhaus et al. (2013); [5] Siebert et al. (2011); [6] Righter et al. (2009); [7] Righter et al. (2010); [8] Righter and Drake (2000); [9] Righter et al. (2008); [10] Capobianco et al. (1999); [11] Jana and Walker (1997c); [12] Walker et al. (1993); [13] Hillgren et al. (1996); [14] Jana and Walker (1997a); [15] Jana and Walker (1997b); [16] Wang et al. (2016).